



Analysis of Ferrite Coplanar Waveguide Transmission Line

M.A. Abdalla^{*}, H.A. Elregaily[†], and A.A. Mitkees[‡]

Abstract: In this paper, we introduce detailed analysis of electromagnetic wave propagation along a planar ferrite coplanar waveguide transmission line. The analysis was done using the electromagnetic full wave of CPW transmission lines implemented on ferrite substrate. All the possible excitation directions of the applied DC magnetic bias were studied. The analytical study was verified using full wave simulations of electromagnetic waves propagation along different types of ferrite coplanar waveguide. The simulation results confirmed the propagation characteristics derived in the analytical study.

Keywords: Ferrite, Coplanar waveguide, Full wave analysis, Permeability

1. Introduction

The need for devices with different magnetic properties requires the use of a magnetic material. Magnetic materials comprise ferromagnetic and ferrimagnetic materials (Ferrites). Examples of ferromagnetic materials are iron and nickel. Ferrites are similar to ferromagnetic materials except ferrites usually have lower saturation magnetizations. Ferrites are found in compounds, with complex crystal structures, whose raw material is turned into powder which can be formed into a hard ceramic material. Ferrites are usually compared in terms of saturation magnetization rather than susceptibility or relative permeability. Also, ferrite is a magnetic anisotropic material whose anisotropy properties are induced by the applying DC magnetic bias field.

Ferrites have a lot of attractive properties for microwave engineering. First, they have tuneable and nonreciprocal properties due to their magnetic properties. Second, as mentioned above, ferrites allow the propagation of electromagnetic within them due to their electrical insulator properties. Also, they have greater electrical resistivity than ferromagnets which introduce much lower eddy current losses. Finally, they can be fabricated in different shapes at low cost techniques. Therefore, ferrites are widely used at microwave frequency applications such as circulators, isolators, and gyrators [2-4]. Thanks to the ferrite electrical insulator properties that ensure total penetration of electromagnetic fields, ferrite substrates are widely used in many dispersive and nonreciprocal microwave magnetic planar circuits depending on the applied DC magnetic bias.

^{*} maaabdallah@gmail.com Dr., Electronic Engineering Department, MTC University, Cairo

[†] Egyptian Armed Forces, Egypt.

[‡] Egyptian Armed Forces, Egypt.

In this paper, we introduce mathematical analysis of electromagnetic wave propagation in a planar ferrite coplanar waveguide (CPW) transmission line. This mathematical study has been done using the electromagnetic full wave analysis of ferrite CPW transmission lines. Such analysis has been explained in details for a ferrite microstrip TL in [1] but have not been formulated in CPW case. The explanation will be introduced in details in this paper for different directions of applied DC magnetic bias.

2. General

It is understood that a microwave signal can propagate through a ferrite differently in different directions, i.e. nonreciprocal propagation, controlled by the applied DC magnetic bias. The relative permeability tensor is dependent on the direction of ferrite magnetization as [3]

$$[\mu] = \begin{bmatrix} \mu & jk & 0 \\ -jk & \mu & 0 \\ 0 & 0 & 1 \end{bmatrix} \quad (\hat{Z} \text{ Bias}) \quad (1)$$

$$[\mu] = \begin{bmatrix} \mu & 0 & -jk \\ 0 & 1 & 0 \\ jk & 0 & \mu \end{bmatrix} \quad (\hat{Y} \text{ Bias}) \quad (2)$$

$$[\mu] = \begin{bmatrix} 1 & 0 & 0 \\ 0 & \mu & jk \\ 0 & -jk & \mu \end{bmatrix} \quad (\hat{X} \text{ Bias}) \quad (3)$$

where

$$\mu = \frac{\omega_{hm}^2 - \omega^2}{\omega_h^2 - \omega^2} \quad (4)$$

$$k = \frac{\omega \omega_m}{\omega_h^2 - \omega^2} \quad (5)$$

The Larmor frequency (gyromagnetic resonance frequency) (ω_h), the magnetization frequency (ω_m), and (ω_{hm}) are defined as

$$\omega_h = \mu_0 \gamma H_0 \quad (6)$$

$$\omega_m = \mu_0 \gamma M_s \quad (7)$$

$$\omega_{hm} = \mu_0 \gamma \sqrt{H_0 (H_0 + M_s)} \quad (8)$$

where γ is the gyromagnetic ratio, the ratio between the spin magnetic moment to the spin angular moment, equals 1.759×10^{11} C/Kg..

3. TEM Mode Propagation in a Normally Magnetized Ferrite CPW TL

In this section, we present the mathematical analysis of a normally magnetized ferrite CPW TL, i.e. magnetized perpendicular to the direction of propagation. For an electromagnetic wave propagating along a ferrite CPW TL, there are two possible normal directions. First, the

DC magnetic bias direction is horizontal, i. e., it is along the CPW strip width. Second, it is vertical which means that it is along the substrate thickness. These two possible DC magnetic bias directions are shown in Figure 1. First, we present the mathematical analysis of the horizontally magnetized ferrite CPW TL while the other case can be considered in similar way. Then, the ferrite TL performance is verified numerically for both normal DC magnetic bias directions.

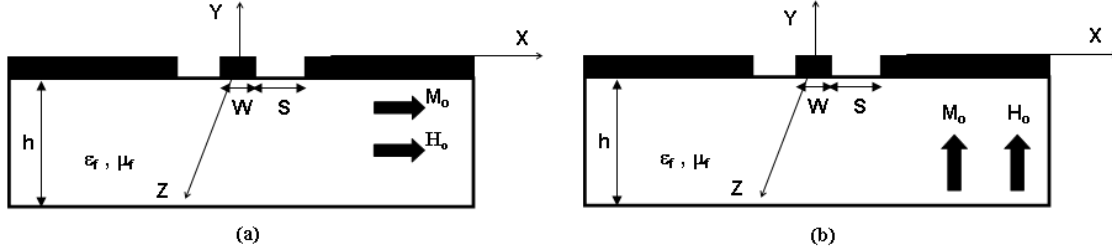


Figure 1 The front view of the CPW TL on ferrite substrate
(a) Horizontally magnetized (b) Vertically magnetized.

TEM Mathematical Analysis

In this section, the full wave analysis technique of Maxwell's equations is used to derive the field components and the propagation parameters of a horizontally biased ferrite CPW TL as shown in Figure 1 (a). The ferrite permeability tensor is expressed as in (3). For simplicity of the analysis, the CPW structure was assumed to be infinite in X and Z directions. Accordingly, the propagating mode was assumed to be TEM mode. Assuming a TEM mode, propagating a long the Z direction with propagation constant γ_z , then the longitudinal components for both electric and magnetic fields (E_z and H_z) are zero. Maxwell's equations can be written as

$$H_x = -\frac{\gamma_z}{-j\omega\mu_o\mu} E_y \quad (9)$$

$$H_y = -\frac{\gamma_z}{j\omega\mu_o} E_x \quad (10)$$

$$\left(\gamma_z^2 + \omega^2\mu_o\epsilon_o\epsilon_r\right)E_x = 0 \quad (11)$$

$$\left(\gamma_z^2 + \omega^2\mu_o\epsilon_o\mu\epsilon_r\right)E_y = 0 \quad (12)$$

From above equations, there are two possible solutions assuming either the field component E_y or E_x is zero.

A- Solution (1)

This solution is based on that $E_y=0$. In this case, the following results are valid:

$$\bar{E} = E_o e^{\gamma_z z} a_x \quad (13)$$

$$\bar{H} = -\frac{\gamma_z E_o}{j\omega\mu_o} e^{\gamma_z z} a_y \quad (14)$$

$$\gamma_z = j\frac{\omega}{c}\sqrt{\epsilon_r} \quad (15)$$

where E_o is the electric field component magnitude. The constants a_x and a_y are two unit vectors in the X and Y directions, respectively. From the field components derived in (13) and

(14), it is clear that this solution presents a TEM mode. The propagation constant shown in (15) indicates that this mode is independent on the magnetic properties of ferrite substrate.

B- Solution (2)

This solution is based on that $E_x=0$. In this case, the following results are valid:

$$\bar{E} = E_o e^{\alpha_x x} e^{\gamma_z z} \hat{a}_y \quad (16)$$

$$\bar{H} = E_o \frac{\gamma_z}{-j\omega\mu_o\mu} e^{\alpha_x x} e^{\gamma_z z} \hat{a}_x \quad (17)$$

$$\gamma_z = j \frac{\omega}{c} \sqrt{\mu\epsilon_r} \quad (18)$$

$$\alpha_x = j \frac{k}{\mu} \gamma_z \quad (19)$$

where E_o is the electric field component magnitude. The field components obtained in (16) and (17) demonstrate the TEM propagation nature of this solution. Also, these two equations illustrate propagation along the Z direction with attenuation along the X direction, parallel to the DC magnetic bias direction. Both of the propagation constant and the attenuation one given in (18) and (19), respectively, are dependent on the ferrite tensor permeability element (μ) that is given in (4). The dispersive nature of (μ) causes the propagating mode to be an evanescent mode when the ferrite tensor permeability is negative. Also, the propagation is lossless along the strip width, a long X direction, with a dispersive attenuation constant according to the value of the ferrite relative permeability tensor element (μ).

It can be concluded that for a positive permeability tensor element, a propagating wave will appear at the end of the ferrite CPW TL. But, for negative permeability, no output signal exists, instead the power is transformed along the strip width direction; i.e. no signal is reflected back.

Similar results for the TEM propagation along a vertically biased ferrite CPW TL, shown in Figure 1 (b) can be obtained with interchanging the field components.

Consequently, the effective relative ferrite permeability for normal DC magnetic bias (μ_{fn}) and hence its negative values frequency band ($f_{nl} < f < f_{nh}$) can be given as

$$\mu_{fn} = \mu \quad (20)$$

$$f_{nl} = \frac{1}{2\pi} \omega_h \quad (21)$$

$$f_{nh} = \frac{1}{2\pi} \omega_{hm} \quad (22)$$

Full Wave Simulations

The aforementioned theoretical study has been verified by simulating the transmission characteristics of a ferrite CPW TL using the electromagnetic full wave simulation for different DC magnetic bias values. The commercial software ANSOFT- HFSS was employed in the simulation. The two possible normal magnetization directions have been examined. The examined ferrite CPW TL in both cases has a strip width $W=3.12$ mm, a slot width $S=1.2$

mm, and a total length of 10 mm. The substrate thickness is $h=1\text{mm}$ and the ferrite substrate has saturation magnetization $4\pi M_S = 1780$ Gauss.

First, assuming that a uniform internal magnetic field H_0 is applied horizontally to a ferrite CPW TL as shown in Figure 1 (a), the simulated transmission characteristics are shown in Figure 2. For $H_0=0$ Oe, in Figure 2 (a), the figure shows that the line has no stopband propagation. The absence of the stopband confirms the analytically derived negative permeability calculation formula introduced in equations (16) to (19) that predicts no negative permeability values for zero internal DC magnetic bias.

For $H_0=500$ Oe, analytically, the calculated negative permeability frequency bandwidth for this DC magnetic bias value, from (20), is within 1.4 GHz to 3.1 GHz. For this case, the simulated transmission characteristics are shown in Figure 2 (b). In the figure, the ferrite TL exhibits a 0 dB insertion loss transmission within the whole studied frequency bandwidth except from 2 GHz to 6.4 GHz, imperfect transmission within this frequency band. The ferrite TL has almost reciprocal lossy propagation, with transmission coefficient level between 0 and -3 dB, within the frequency band from 2 GHz to 2.6 GHz. Then, it demonstrates a significant nonreciprocal stopband within the frequency band from 2.6 GHz to 3.2 GHz. This stopband is characterized by both of low reflection coefficient, almost better than -10 dB, and low transmission coefficient, lower than -10 dB for S_{12} magnitude. Finally, the TL has a reciprocal lossy propagation in the bandwidth that extends from 3.6 GHz to 6 GHz. By comparing the nonreciprocal stopband bandwidth with the analytically calculated bandwidth of negative permeability, we can comment that the analytical calculation can predict to high degree of accuracy the upper cut off frequency of simulated nonreciprocal stopband. However, it introduces a lower shift for the lower cut off frequency.

Similar results can be obtained for $H_0=1000$ Oe and 2000 Oe, as shown in Figure 2 (c) and (d), respectively. For $H_0=1000$ Oe, the whole imperfect transmission bandwidth extends from 3.3 GHz to 7.8 GHz where its nonreciprocal stopband is within the frequency band 3.8 GHz to 4.7 GHz. Also, it is noted that its lower cut off frequency, 3.8 GHz, is higher than the analytically calculated one, 2.8 GHz whereas its upper cut off frequency, 4.7 GHz is close to the analytically calculated one, 4.8 GHz. For $H_0=2000$ Oe, the simulated nonreciprocal propagation stopband is within 6.5 GHz to 7.7 GHz while the analytically calculated one is within 5.6 GHz to 7.7 GHz.

It can be seen from these two cases that low levels for both of the reflection coefficient (S_{11}) and the transmission coefficients (S_{12} and S_{21}) within the negative ferrite permeability stopband decrease by increasing the DC magnetic bias value. Also, it is observed that the nonreciprocal propagation properties become more significant by increasing the DC magnetic bias.

From all the above studied cases, we can conclude that the ferrite TL has negative permeability within the frequency bandwidth whose lower cut off frequency is slightly higher than f_{nl} defined in (21) and its upper cut off frequency coincides approximately with f_{nh} defined in (22). This verifies the TEM mathematical analysis introduced above for the horizontal DC magnetic bias direction. The variations of cut off frequencies are due to the approximation done in the analytical calculation.

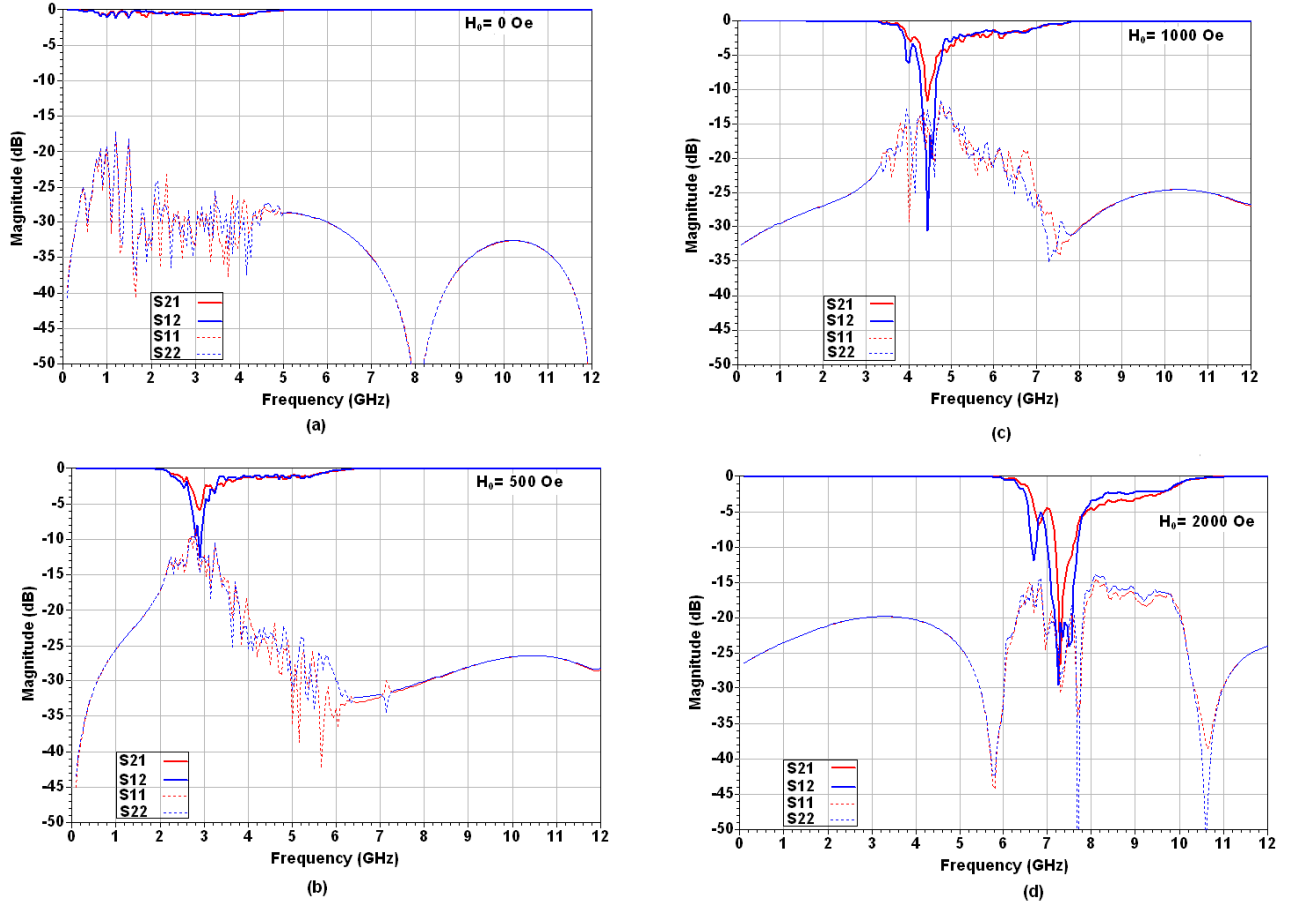


Figure 2 The full wave scattering parameter magnitudes of the ferrite CPW TL for (a) $H_0=0$ Oe, (b) $H_0=500$ Oe, (c) $H_0=1000$ Oe, and (d) $H_0=2000$ Oe horizontal biased.

The second step in the numerical study is to verify the vertically magnetized ferrite CPW TL analytical study. Thus, the same ferrite CPW TL with vertical magnetization is simulated using HFSS for the same DC magnetic bias values as shown in Figure 3. It is worth to repeat that the vertically magnetized ferrite CPW TL has the analytically derived definition of relative permeability in (20), similar to the horizontal magnetization case.

First, for $H_0=0$ Oe, it is clear from its simulated scattering parameters in Figure 3 (a), that the ferrite CPW TL has no stopband propagation. This confirms the theoretical analysis of the vertically magnetized ferrite CPW TL which implies that its relative permeability, defined in (20), is always positive for zero DC magnetic bias.

Next, the simulated scattering magnitudes for $H_0=500$ Oe, 1000 Oe, and 2000 Oe are shown in Figure 3 (b), (c), and (d), respectively. As shown in these figures, the ferrite CPW TL illustrates dispersive lossy propagation with clear stopband and insignificant nonreciprocal properties for all these cases. For $H_0=500$ Oe, the whole imperfect transmission extends from 1.5 GHz to 5 GHz with higher insertion loss within the frequency band from 1.8 GHz to 2.5 GHz. For $H_0=1000$ Oe, the whole imperfect transmission extends from 2.8 GHz to 7.4 GHz with higher insertion loss within the frequency band from 3.2 GHz to 4 GHz. Finally, for $H_0=2000$ Oe, the whole imperfect transmission extends from 5.4 GHz to 10 GHz with higher insertion loss within the frequency band from 5.6 GHz to 7.3 GHz.

From these studied cases, we can conclude that, the introduced significant stopband is characterized by low reflection and transmission coefficients, similar to the horizontal magnetization ferrite CPW TL case. However, in comparison with horizontal magnetization, the vertical case has higher reflection coefficient and higher transmission coefficients. By comparing the stopband bandwidth, with the analytically calculated bandwidth of negative permeability, we observe that the analytical calculation introduces both positive and negative shifts for the lower and upper cut off frequencies of the simulated stopbands, respectively. It is observed that these two shifts decrease, specially the positive shift, by increasing the DC magnetic bias values. For $H_0=2000$ Oe the analytically derived permeability is expected to be negative starting from 5.6 GHz, which coincides exactly with the numerical found value, and lasting to 7.7 GHz which is 0.4 GHz higher than the numerically found one.

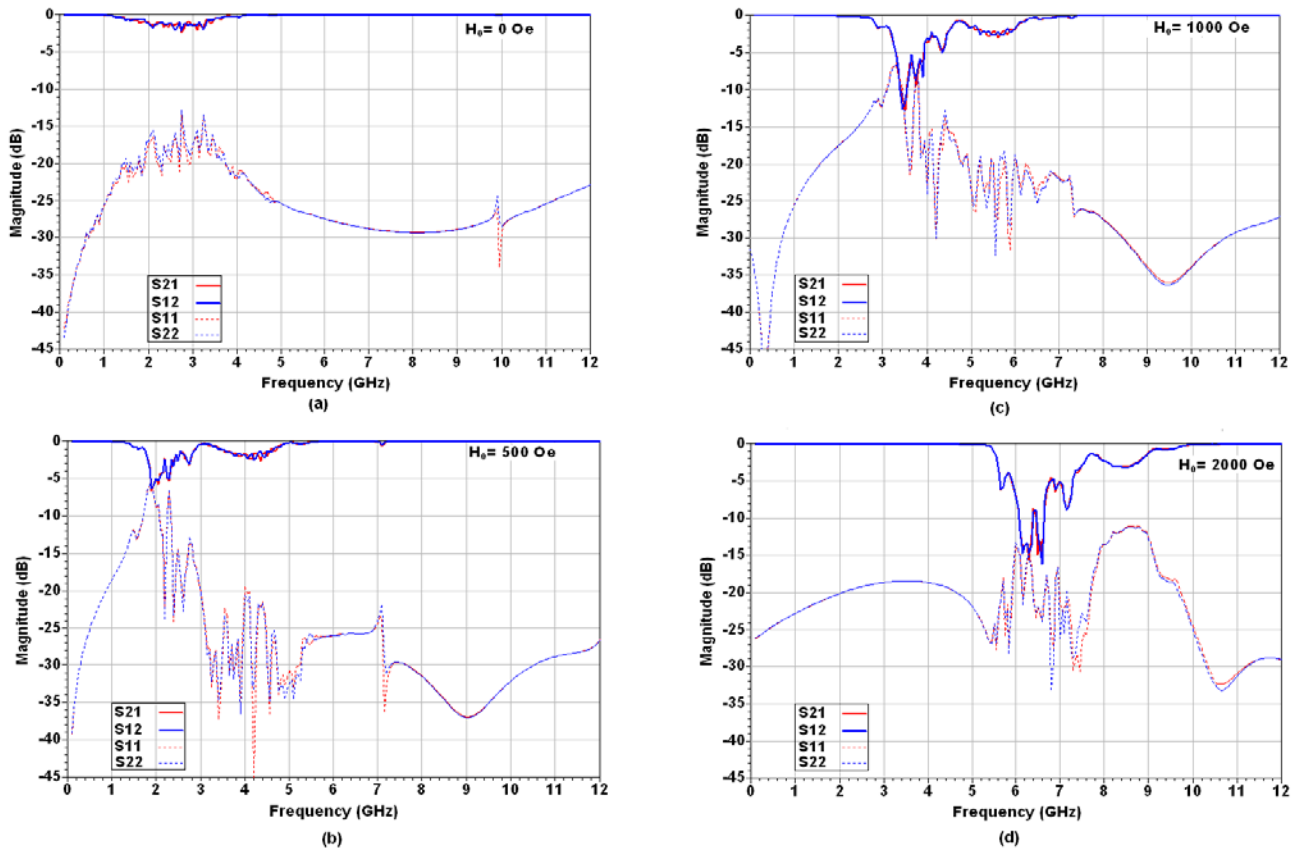


Figure 3 The full wave scattering parameter magnitudes of the ferrite CPW TL for (a) $H_0=0$ Oe, (b) $H_0=500$ Oe, (c) $H_0=1000$ Oe, and (d) $H_0=2000$ Oe vertically biased.

4. TEM Mode Propagation in a Longitudinally Magnetized Ferrite CPW TL

In this section, we present the study of the longitudinally biased ferrite CPW TL, i.e. magnetized along the direction of propagation. The front view of the ferrite CPW TL is shown in Figure 4. First, we introduce its mathematical analysis and then this analysis will be verified numerically by studying its scattering parameters.

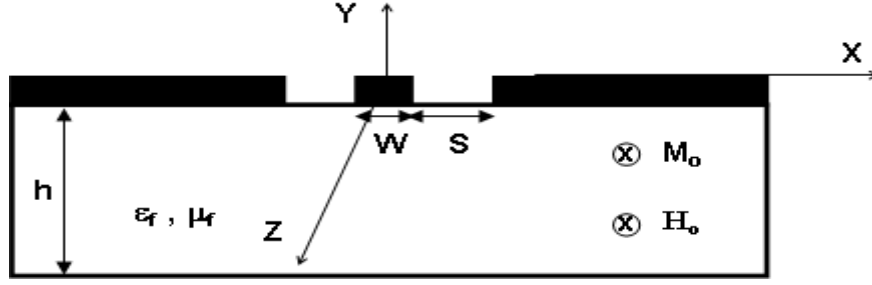


Figure 4 The front view of the ferrite CPW TL, longitudinally magnetized.

TEM Mathematical Analysis

The mathematical analysis of the longitudinally magnetized ferrite CPW TL can be done similar to the aforementioned analysis for normal biased ferrite CPW TL using the full wave analysis technique. For this DC magnetic bias, the permeability tensor of CPW transmission line biased in Z direction defined in (1).

Similar to normal analysis, assume a TEM mode, propagating along the Z direction with propagation constant γ_z , then the longitudinal components for both electric and magnetic fields (E_z and H_z) are zero. Thus, Maxwell's equations can be written as

$$H_x = -\frac{j\omega\epsilon}{\gamma_z} E_y \quad (23)$$

$$H_y = \frac{j\omega\epsilon}{\gamma_z} E_x \quad (24)$$

$$(-j\omega^2 \mu_o \epsilon_o \epsilon_r k) E_x + (\gamma_z^2 + \omega^2 \mu_o \mu \epsilon_o \epsilon_r) E_y = 0 \quad (25)$$

$$(\gamma_z^2 + \omega^2 \mu_o \mu \epsilon_o \epsilon_r) E_x + (j\omega^2 \mu_o \epsilon_o \epsilon_r k) E_y = 0 \quad (26)$$

Solving the two equations set (25) and (26), we can find that there are two possible solutions with two different propagation constants; which can expressed as

$$\gamma_{z1} = j\omega\sqrt{\mu_o \epsilon_o \epsilon_r (\mu - k)} \quad (27)$$

$$\gamma_{z2} = j\omega\sqrt{\mu_o \epsilon_o \epsilon_r (\mu + k)} \quad (28)$$

The two electric field components (E_1) and (E_2), associated with γ_{z1} and γ_{z2} , respectively, are

$$E_1 = E_o (\hat{a}_x - j\hat{a}_y) e^{-\gamma_{z1} z} \quad (29)$$

$$E_2 = E_o (\hat{a}_x + j\hat{a}_y) e^{-\gamma_{z2} z} \quad (30)$$

where E_o is the electric field component magnitude. The final expression for the propagated electric field components in (29) and (30), confirms that propagation is TEM mode. Also, it can be claimed that the propagation mode has lossless propagation constant along the propagation direction (Z). However, this propagation constant is dependent on both of the

ferrite tensor parameters μ and k given in (4) and (5), respectively. Therefore, it is expected that the propagation will have a dispersive nature based on the applied DC magnetic bias value. On contrast to the normal DC magnetic bias case explained previously, the propagation has no attenuation along DC magnetic bias direction. In other words, for positive effective permeability frequency band, lossless propagation along the TL exists. But, for negative permeability frequency band, no propagation along that direction and the input signal will be reflected back.

A formula for the effective relative ferrite permeability of longitudinal magnetization can be defined using duality with the longitudinal magnetized ferrite microstrip TL [5] or ferrite slab [6] as

$$\mu_{fp} = \frac{\mu^2 - k^2}{\mu} = \frac{(\omega_h + \omega_m)^2 - \omega^2}{\omega_{hm}^2 - \omega^2} \quad (31)$$

It is shown that the effective permeability has a dispersion nature whose value is negative or positive depending on the properties of the ferrite substrate and the applied DC magnetic bias. This equivalent permeability will be negative values for the frequency range $f_{pl} < f < f_{ph}$ given as follow

$$f_{pl} = \frac{1}{2\pi} \omega_{hm} \quad (32)$$

$$f_{ph} = \frac{1}{2\pi} (\omega_h + \omega_m) \quad (33)$$

Full Wave Simulation

The theoretical study of longitudinally magnetized ferrite CPW TL was verified numerically by simulating such TL using HFSS. The simulated ferrite CPW TL has the same dimensions and ferrite substrate properties as assumed in the normal magnetization analysis. It is noted that, the definition of the relative permeability of longitudinal magnetized case is given in (31).

The simulating scattering parameters for such TL for different DC magnetic bias values are shown in Figure 5. From the figure, it can be observed that the ferrite CPW TL illustrates dispersive non propagation bandwidths with very dominant stopband and almost reciprocal properties for all studied cases, including $H_0=0$ Oe case. Also, unlike the two normally magnetized cases, this stopband is characterized by both of very high reflection coefficient and low transmission coefficient. Approximately, at centre frequencies of such stopband, the reflection coefficient is higher than -5 dB in all cases while the transmission coefficient is lower than -25 dB in all cases except zero bias case where it is a bit lower than -10 dB.

The simulated scattering parameters for $H_0=0$ Oe is shown in Figure 5 (a). Unlike, to the normal magnetized cases, a significant stopband exists in the frequency band 1.7 GHz to 3.25 GHz with almost -5 dB reflection coefficient. Within this stopband the transmission coefficient are below -5 dB and it goes below -15 dB at 2.8 GHz. Below this stopband, from 1 GHz to 1.7 GHz, and higher than it, from 3.25 GHz to 5 GHz, the TL demonstrates lossy propagation with transmission coefficient lower than -5 dB and approximately -10 dB reflection level. The stopband appearance confirms the permeability definition in (31) which implies that it is negative for zero longitudinal DC magnetic bias within the frequency band

from $f_{pl} = 0$ to $f_{ph} = 5$ GHz as calculated from (32) and (33), respectively. However, a significant variation between these two cut off frequencies obtained either analytically or numerically which will be analyzed in more details for the higher DC magnetic bias cases.

The simulated scattering magnitudes for $H_0 = 500$ Oe, 1000 Oe, and 2000 Oe are shown in Figure 5 (b), (c), and (d), respectively. As shown in the figures, the significant stopband extends from 3.4 GHz to 6.4 GHz for $H_0 = 500$ Oe, from 4.7 GHz to 7.7 GHz for $H_0 = 1000$ Oe, and from 7.4 GHz to 10.6 GHz for $H_0 = 2000$ Oe. All these stopbands have S_{11} level higher than -5 dB and very low reciprocal S_{21} level, reaches -25 dB at center operating frequencies, frequencies of maximum reflection coefficient and minimum transmission coefficient. On the other hand, analytically derived bandwidth of negative permeability ($f_{pl} < f < f_{ph}$) calculated from (32) and (33), respectively for these DC magnetic bias values are as follow. For $H_0 = 500$ Oe, this bandwidth extends from 3 GHz to 6.4 GHz, for $H_0 = 1000$ Oe, it extends from 4.7 GHz to 7.8 GHz, and it is from 7.7 GHz to 10.6 GHz for $H_0 = 2000$ Oe.

By comparing the two bandwidth values, we can conclude that the ferrite TL has negative permeability within the frequency band whose lower cut off frequency is close to f_{pl} defined in (32) while its upper cut off frequency coincides approximately with f_{ph} defined in (33).

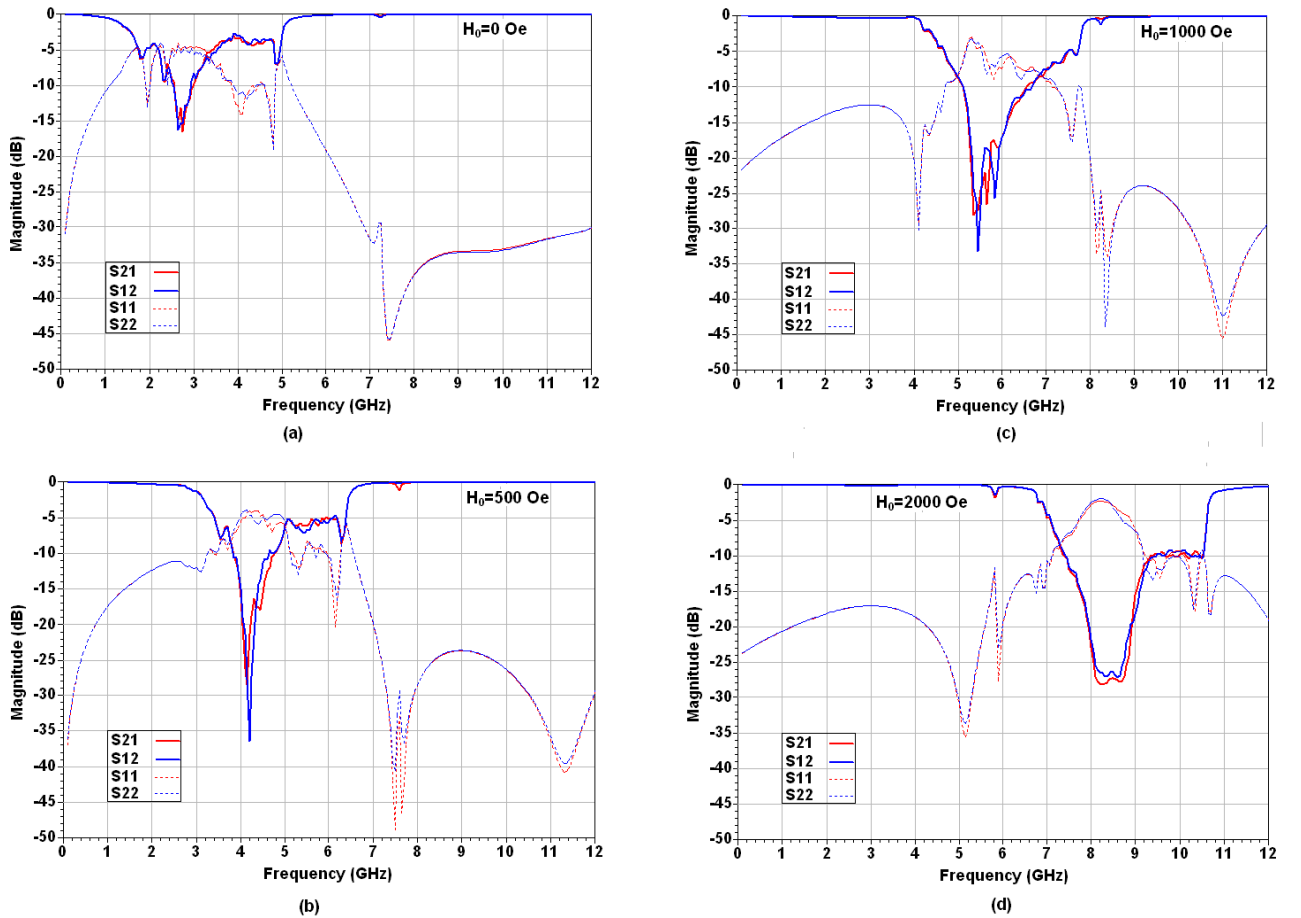


Figure 5 The full wave scattering parameter magnitudes of ferrite CPW TL for (a) $H_0 = 0$ Oe, (b) $H_0 = 500$ Oe, (c) $H_0 = 1000$ Oe, and (d) $H_0 = 2000$ Oe longitudinally biased.

References

- [1] M. E. Hines, "Reciprocal and nonreciprocal modes of propagation in ferrite stripline and microstrip devices," *IEEE Transactions on Microwave Theory and Techniques*, vol. MTT-19, pp. 442-51, 1971.
- [2] R. A. Waldron, *Ferrites : an introduction for microwave engineers*. New York: Van Nostrand, 1962.
- [3] D. M. Pozar, *Microwave engineering*. New York: J. Wiley & Sons, 1998
- [4] A. J. B. Fuller, *Ferrite at microwave frequencies*. Stevenage, London: Institution of Engineering and Technology, 1987
- [5] C. S. Teoh and L. E. Davis, "Normal-mode analysis of ferrite-coupled lines using microstrips or slotlines," *IEEE Transactions on Microwave Theory and Techniques*, vol. 43, pp. 2991-2998, 1995.
- [6] G. Dewar, "A negative index of refraction metamaterial based on a wire array embedded in ferrite," presented at Complex Mediums VI: Light and Complexity, Jul 31-Aug 2 2005, San Diego, CA, United States, 2005.